ARTICLES

Photoinduced Electron-Transfer Processes between [C60]Fullerene and Triphenylamine Moieties Tethered by Rotaxane Structures. Through-Space Electron Transfer via Excited Triplet States of [60]Fullerene

Atula S. D. Sandanayaka,[†] Hisahiro Sasabe,[‡] Yasuyuki Araki,[†] Yoshio Furusho,[‡,§] Osamu Ito,*[,†] and Toshikazu Takata*[,‡,||]

Institute of Multidisciplinary Research for Advanced Materials, Tohoku University, Katahira 2-1-1, Aoba-ku, Sendai 980-8577, Department of Organic and Polymeric Materials, Tokyo Institute of Technology, O-okayama, Meguro-ku, Tokyo 152-8552, and Department of Applied Chemistry, Osaka Prefecture University, 1-1 Gakuen-cho, Sakai-shi, Osaka 599-8531, Japan

Received: March 1, 2004

Two rotaxanes tethering [60]fullerene (C_{60}) and triphenylamine (TPA) moieties were synthesized in good yields by the urethane end-capping method using a crown ether−secondary amine motif. In these rotaxanes, the C_{60} group serving as electron acceptor is attached to the crown ether wheel through which the axle with a TPA group acting as electron donor on its terminal penetrates. One rotaxane has an ammonium moiety, whereas the other has a neutral amide moiety in the center of the axle. The corresponding reference compounds without rotaxane structures were also prepared. The intra-rotaxane photoinduced electron-transfer processes of C_{60} and TPA have been investigated by time-resolved transient absorption and fluorescence measurements with changing solvent polarity and temperature. Nanosecond transient absorption measurements of these rotaxanes demonstrated that the long-lived charge-separated state $(C_{60}^{\bullet-},TPA^{\bullet+})_{rotaxane}$ is formed via the excited triplet state of C_{60} ($^3C_{60}$*) in polar solvents. The rate constants for the charge separation process were in the range of $(5-8) \times 10^7$ s^{-1}, while the rate constants of charge recombination were in the range of $(3-6) \times 10^6$ s^{-1}, corresponding to the lifetimes of the charge-separated states of 170−300 ns. Both rate constants depended on rotaxane structure, solvent polarity, and temperature. The activation free energy changes of charge separation and recombination processes were evaluated to be 0.01−0.03 and 0.03−0.06 eV by temperature dependences, respectively. Such low activation energies may be related to through-space electron transfer in these rotaxanes. On the other hand, in a covalently connected TPA−C_{60} dyad, fast charge separation from the excited singlet state and fast charge recombination were observed through bonds in polar solvents.

Introduction

Supramolecular fullerene chemistry is a rapidly emerging field with fascinating scientific and technological perspectives.[1−3] The excited-state properties of fullerene derivatives in the supramolecules have attracted interest in studies of photosynthesis models, as well as studies directed toward the development of new photovoltaic devices and photodetectors.[4,5] In addition, the unique geometry of the supramolecules provides templates with enormous scope for a variety of studies including investigations of energy- and electron-transfer processes within the supramolecular assemblies containing fullerenes under photoillumination.[6] Covalently bonded molecules with donor−acceptor systems involving electron-mediating and hole-transfer reagents have been extensively studied to establish rapid and efficient charge separation (CS) via the excited singlet state of fullerene derivatives and donor molecules, resulting in long-lived charge-separated states.[7−11] Other supramolecules composed of the coordination bonds between fullerene derivatives appending nitrogen atoms and zinc porphyrins have also been shown to display fast and effective CS processes via the excited singlet state of fullerene derivatives and donor molecules.[12−16]

Recently, rotaxanes containing fullerenes as electron acceptors and phthalocyanine and porphyrin as electron donors were synthesized, whereby fullerenes were spatially fixed with respect to the phthalocyanine and porphyrin moieties. It was reported that, in these rotaxanes, the CS process takes place via the singlet excited states of these chromphores.[17,18]

In the present study, we synthesized two fullerene rotaxanes with a triphenylamine (TPA) moiety as electron donor. Figure 1 shows the structures of these rotaxanes (abbreviated as [2]rotaxanes **1** and **2**), in which the axle connecting the TPA donor moiety at the one end penetrates through the crown ether wheel attached to a [60]fullerene (C_{60}) acceptor. In **1**, the nitrogen atom in the middle of the axle has a positive charge and is expected to interact with oxygen atoms of the crown

* To whom correspondence should be addressed. E-mail: ito@tagen.tohoku.ac.jp (O.I.); ttakata@polymer.titech.ac.jp (T.T.).
† Tohoku University.
‡ Osaka Prefecture University.
§ Present address: Yashima Super-Structured Helix Project, JST, Moriyama-ku, Nagoya 552-8555, Japan.
|| Tokyo Institute of Technology.

10.1021/jp0490812 CCC: $27.50
Published on Web 05/20/2004

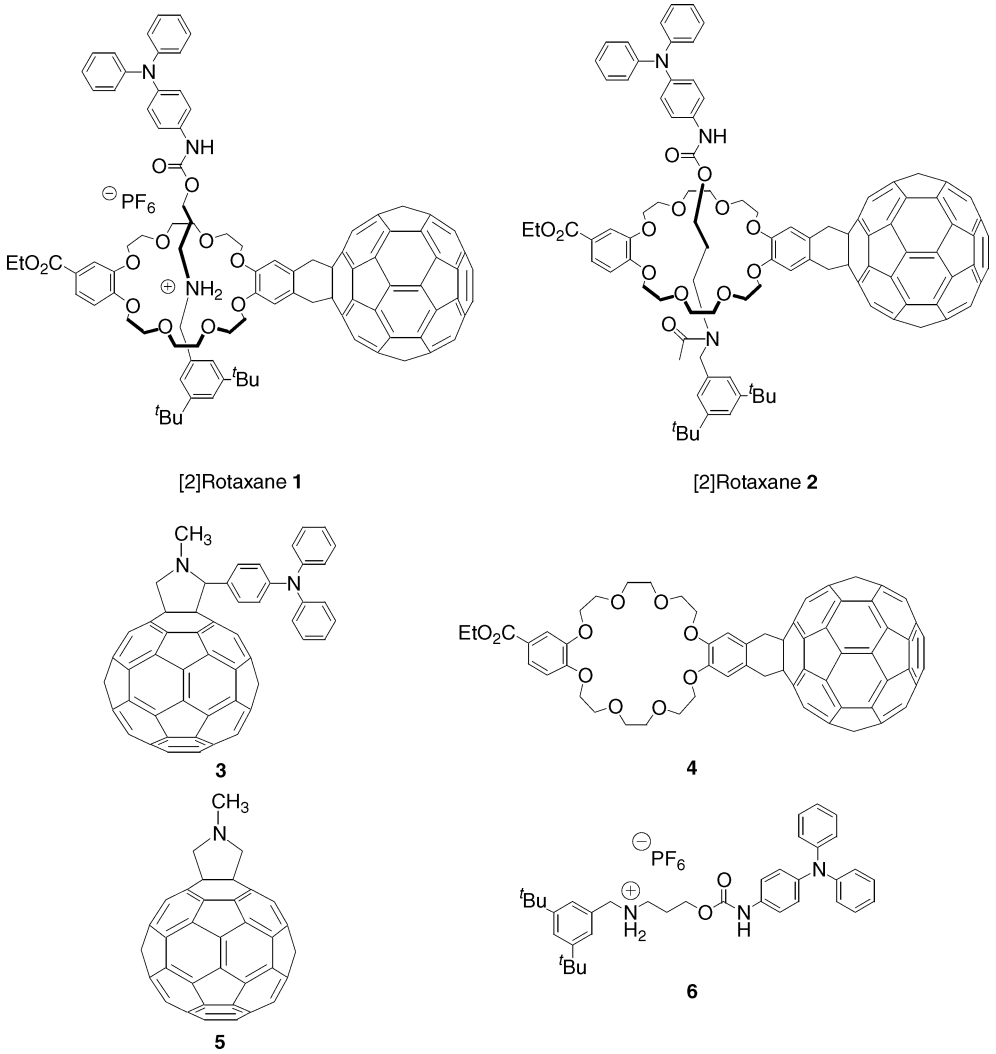

Figure 1. Molecular structures of [2]rotaxanes (C_{60},TPA) and references.

ether, probably fixing the fullerene and TPA moieties in a certain spatial arrangement. In **2**, the axle has a neutral amide group in the center, resulting in mobility of the axle with respect to the wheel. These rotaxanes are novel fullerene rotaxanes that were first prepared by utilizing the crown ether−secondary ammonium motif. Related compounds **3**−**6** were used as reference compounds.

For these two rotaxanes, we examined the photoinduced processes using time-resolved transient absorption and fluorescence measurements with varying solvent polarity and temperature. In the past decade, photoinduced electron-transfer (ET) processes for fullerene−amine systems have gained great attention, and a vast variety of fullerene−amine dyads, triads, and more complex systems have been synthesized and investigated.[19−21] In most covalently connected dyad systems of fullerenes and amines, excitation of the fullerene initiates ET from the excited singlet state of C_{60} ($^1C_{60}$*) moiety, generating CS states ($C_{60}^{\bullet-}$−amine$^{\bullet+}$) with relatively short lifetimes of a few nanoseconds.[19,20]

In general, in fullerene−amine mixture systems, photoinduced ET mainly occurs via the excited triplet state of C_{60} ($^3C_{60}$*), producing long-lived radical ions when the amine concentrations are sufficiently low in polar solvents.[22,23] On the other hand, in high amine concentrations, photoinduced ET mainly occurs via $^1C_{60}$*, producing short-lived radical ion pairs ($C_{60}^{\bullet-}$−amine$^{\bullet+}$) in nonpolar solvents.[24,25]

The aim of this study is to compare these reported photoinduced ET processes in the fullerene−amine mixture and covalently connected dyads with the photoinduced processes of newly synthesized rotaxanes **1** and **2**, in which through-space ET would be anticipated.

Results and Discussion

Design, Preparation, and Characterization of [2]Rotaxanes 1 and 2. [2]Rotaxanes **1** and **2** were designed to spatially arrange C_{60} and TPA moieties at an appropriate distance for intramolecular ET in the excited state, but not for interaction in the ground state. [2]Rotaxanes **1** and **2** can be synthesized by the end-capping method via a tin-catalyzed urethane-forming reaction.[26] To introduce a C_{60} moiety to **1** and **2**, crown ether **4** bearing a C_{60} moiety was designed. To achieve high solubility of **4** in nonpolar organic solvents such as chloroform, a carboethoxy group was attached to the benzene ring of **4**. A TPA unit was linked to the axle end by a urethane bond.

The synthetic route of **1** and **2** is outlined in Scheme 1. The bromomethylation[27] of carboethoxy-substituted DB24C8 **7**[28] was carried out with an excess amount of formaldehyde and a 40% hydrogen bromide solution in acetic acid at 45 °C to afford the corresponding bis(bromomethyl) derivative **8** in 47% yield. The Diels−Alder reaction[29] of **8** with 1.3 equiv of C_{60} proceeded in refluxing toluene in the presence of a large excess of KI and

SCHEME 1

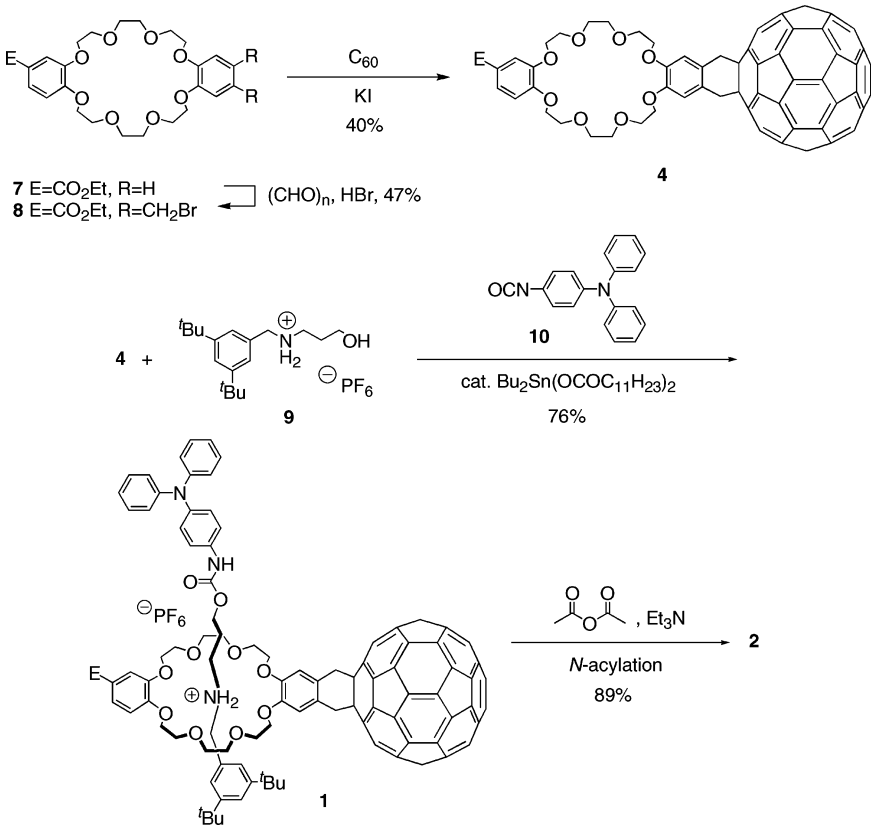

SCHEME 2

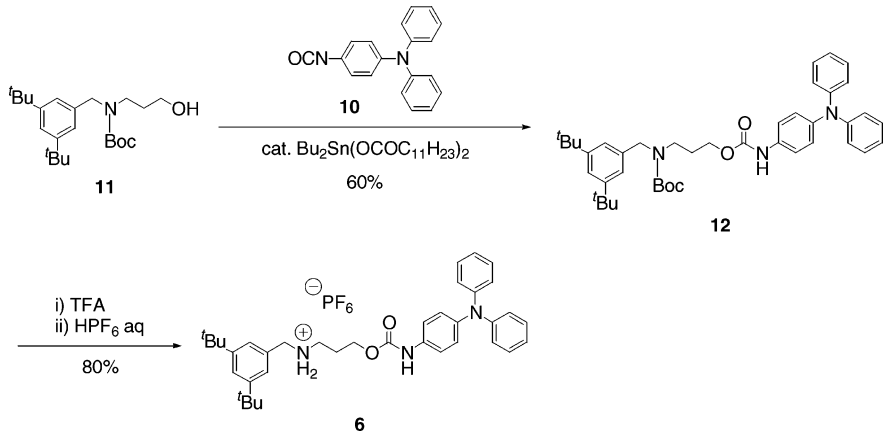

18-crown-6 to give **4** in 40% yield. Crown ether **4,** purified by preparative GPC (eluent chloroform), was highly soluble in chloroform (>400 mg/mL). A chloroform solution of **9**[30] and a slight excess of **4** were treated with 1.5 equiv of isocyanate **10** and 10% dibutyltin dilaurate at room temperature to end-cap the terminal hydroxy group. The target [2]rotaxane **1** thus formed was easily isolated by preparative GPC (eluent chloroform) in 76% yield. The conversion of **1** to neutral acylated [2]rotaxane **2** was achieved in 89% yield[31] by treatment with 3.3 equiv of triethylamine and 3.0 equiv of acetic anhydride in acetonitrile at room temperature. Both [2]rotaxanes **1** and **2** were highly soluble in ordinary organic solvents such as chloroform.

The characterization of rotaxanes **1** and **2** and crown ether **4** was established on the basis of FAB-mass, NMR, IR, and elemental analyses. All displayed the molecular ion peaks corresponding to the designed products in the FAB-mass spectra.

Preparation and Characterization of Axle 6. The axle with TPA moiety **6** at its terminal was synthesized from **11**[32] as shown in Scheme 2. Tin-catalyzed acylation of **11** with 4-(diphenylamino)phenyl isocyanate (**10**) gave *N*-protected axle **12** in 60% yield. Deprotection with trifluoroacetic acid (TFA) was followed by neutralization with aqueous K_2CO_3. The resulting free amine was triturated with aqueous HPF_6 solution to afford hexafluorophosphate **6** in 80% yield. The structure of **6** was confirmed by FAB-mass, NMR, IR, and elemental analyses.

Optimized Structure. By MM2 force field calculations, an optimized structure of *N*-acetylated rotaxane **2** was obtained (Figure 2). The optimized structure, clearly showing a penetrating interlocked structure, seems to indicate the predominant position of the wheel placed on the axle of **2**. In fact, the wheel of **2** is considered to be located mainly at the position nearer to the TPA moiety by *N*-acetylation of **1**, as postulated from the X-ray crystal structures and the structures estimated by ^{1}H NMR of both ammonium-type rotaxane-like **1** and *N*-acetylated rotaxane-like **2**.[31]

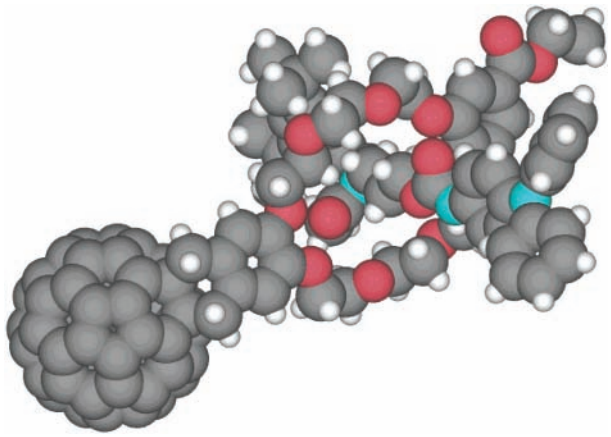

Figure 2. Optimized structure of [2]rotaxane **2** by MM2.

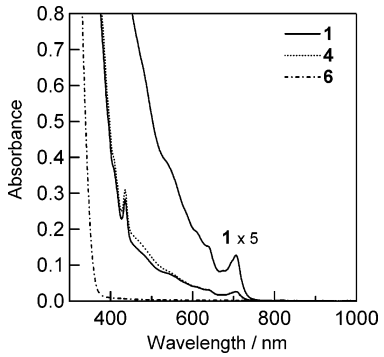

Figure 3. Steady-state absorption spectra of [2]rotaxane **1** (0.1 mM), **4** (0.1 mM), and **6** (0.1 mM) in toluene.

The center to center distance between C_{60} and TPA (R_{cc}) moieties was estimated to be 17 Å from the optimized structure. Similarly, in the case of **1**, the crown wheel locates exclusively at the nitrogen of the axle, and therefore, the R_{cc} value (21 Å) would presumably be slightly longer than that of **2**.

Steady-State Absorption Studies. Figure 3 shows the steady-state absorption spectra of [2]rotaxane **1**, reference C_{60}−crown **4**, and reference axle component **6** in toluene. Absorption bands of the C_{60} moiety appeared both at 705 nm and below 350 nm. Since the absorption spectrum of [2]rotaxane **1** is almost a superimposition of references **4** and **6**, there is no interaction in the ground state between the two elements of [2]rotaxane **1**. Similar results were obtained with [2]rotaxanes **1** and **2** in toluene, THF, benzonitrile (PhCN), and DMF. For a covalently bonded C_{60}−TPA dyad (**3**), the absorption spectrum was slightly changed from a superposition of the TPA and $NMPC_{60}$ (**5**), to ensure a weak interaction in the ground state. In the present study, the laser excitation of [2]rotaxanes **1** and **2** and reference compounds was carried out at 532 nm. Since TPA does not show substantial absorbance at this wavelength, predominant excitation of the C_{60} moiety was possible.

On addition of $FeCl_3$ to TPA axle **6** in PhCN, the absorption band appeared at 742 nm (Figure 4), which can be attributed to the cation radical of the TPA moiety ($TPA^{\bullet+}$) of **6**. Normally, the radical cation of unsubstituted TPA exhibits absorption at around 650 nm.[33] The absorption peak shift to 740 nm in **6** can be explained by the fact that the TPA moiety was substituted with the N atom of the amide group. In fact, the absorption at 740 nm was similarly observed for [2]rotaxanes **1** and **2** by the chemical oxidation with $FeCl_3$. From the amount of added $FeCl_3$, the extinction coefficient (ϵ_{740nm}) of the absorption peak of $TPA^{\bullet+}$ of **6** was evaluated as 29100 M^{-1} cm^{-1}, which is a value similar to that of unsubstituted $TPA^{\bullet+}$.[33]

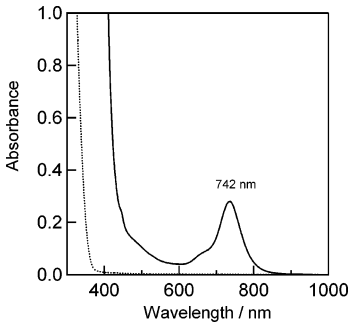

Figure 4. Steady-state absorption spectra of **6** (0.2 mM) in the absence (dashed line) and in the presence (0.4 mM, solid line) of Fe^{3+} in PhCN.

Electrochemical Studies. By cyclic voltammetric measurements, the first reduction (E_{red}) and oxidation (E_{ox}) potentials of [2]rotaxanes **1** and **2** were estimated to be −0.88 and +0.44 V and −0.87 and +0.43 V vs Ag/AgCl in PhCN, respectively. The former negative potentials are attributed to the E_{red} values of the C_{60} moiety, and the latter positive potentials to the E_{ox} values of the TPA moiety in **1** and **2** by comparing E_{red} of the C_{60} moiety in **4** (−0.86 V vs Ag/AgCl) and E_{ox} of the TPA moiety in **6** (+0.54 V vs Ag/AgCl) in PhCN. In the case of covalent dyad **3**, the E_{red} values of the C_{60} moiety and the E_{ox} values of the TPA moiety were evaluated to be −0.88 and +0.70 V vs Ag/AgCl, respectively. An appreciable difference in E_{ox} values of the TPA moiety was observed, suggesting the presence of weak interaction between the C_{60} and TPA moieties in the ground states of **3**. The CS state energy levels, which are equivalent to the free energy of charge recombination (CR) (ΔG_{CR}), were determined by assessing the difference between the E_{ox} and E_{red}, adding the Coulomb energy by the Weller equation.[34] The free energy changes for charge separation (ΔG_{CS}) can be calculated by considering the energy levels of the least excited states of the C_{60} moiety.[35]

Steady-State Fluorescence Studies. The steady-state fluorescence spectra of [2]rotaxane **2** and reference C_{60}−crown **4** were measured in toluene, DMF, PhCN, and THF with excitation at 500 nm (Figure 5a). The fluorescence peak at 715 nm is attributed to that of the C_{60} moiety in rotaxane **2** judging from the fluorescence peak of **4**. Similar fluorescence spectra were observed for **1**. Comparing the fluorescence peak with the absorption peak (709 nm), it became apparent that [2]rotaxanes **1** and **2** showed small Stokes shifts and had the lowest singlet excited energy at 1.75 eV.

The fluorescence intensity of **2** in toluene was only slightly weaker than that of **4**. Fluorescence intensity in THF was much weaker than that in toluene, whereas the quenching of fluorescence intensity in DMF and PhCN was quite smaller than that in THF. A similar tendency was observed for **2**. These observations suggest that the excited singlet state of the C_{60} moiety was not greatly influenced by the TPA moiety in the rotaxanes even in polar solvents except for THF. On the other hand, it is interesting to note that the fluorescence intensity of covalently connected C_{60}−TPA dyad **3** in polar solvents was significantly lower than in the less polar solvent toluene and also than that of reference fullerene derivative **5** (Figure 5b). These observations suggest that CS predominantly takes place from the excited singlet state of the C_{60} moiety in **3**. Further quantitative analyses on the fluorescence properties were subsequently carried out on the basis of lifetime measurements.

Fluorescence Lifetime Measurements. The fluorescence lifetimes (τ_F) of [2]rotaxanes **1** and **2** and reference C_{60}−crown **4** were measured using a time-correlated single-photon-counting

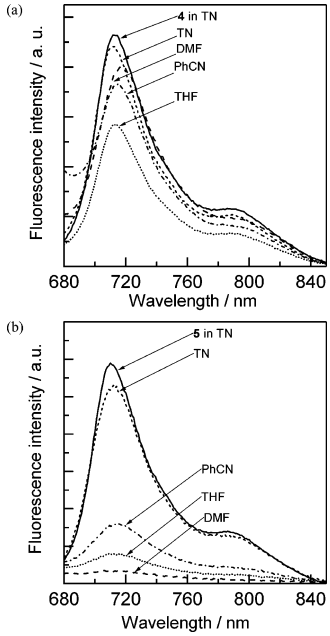

Figure 5. Steady-state fluorescence spectra of (a) [2]rotaxane **2** and reference **4** (0.1 mM) in DMF, PhCN, THF, and toluene (TN) and (b) **3** and reference **5** (0.1 mM) in DMF, PhCN, THF, and TN ($\lambda_{ex} = 500$ nm).

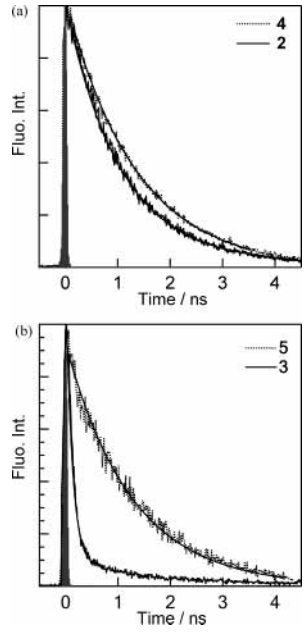

Figure 6. Fluorescence decays of (a) [2]rotaxane **2** and reference **4** and (b) **3** and reference **5** at 715 nm in PhCN. The excitation wavelength was 410 nm.

apparatus with excitation at 410 nm. The time profiles of the fluorescence intensities of **2** and **4** in PhCN are shown in Figure 6a; they are curve-fitted by a single-exponential decay. Similar time profiles of the fluorescence intensities of [2]rotaxanes and **4** were observed in toluene, DMF, PhCN, and THF. The fluorescence lifetimes (τ_F) of the C_{60} moieties in **1** and **2** were evaluated by the curve-fitting method and are listed in Table 1. In toluene, the τ_F values of **1** and **2** were nearly equal to that of **4** (1130 ps). In polar solvents such as PhCN and THF, slightly shorter τ_F values of **1** and **2** than those of **4** (1330 and 1230 ps, respectively) were obtained. In DMF, on the other hand, the τ_F values of **1** and **2** were slightly larger than those of **4**. As a whole, the differences in the τ_F value between the [2]rotaxanes and **4** were small in all solvents employed. From these τ_F values,

TABLE 1: Fluorescence Lifetimes (τ_F), Rate Constants (k_q^S), Quantum Yields (Φ_q^S), and Free-Energy Changes (ΔG_{CS}^S) of Charge Separation of [2]Rotaxanes 1 and 2 in Toluene, THF, PhCN, and DMF at Room Temperature

compd	solvent	τ_F/ps	k_q^S [a]/s^{-1}	Φ_q^S [a]	$-\Delta G_{CS}^S$ [b]/eV
1	toluene	1120	c	c	−0.33
	THF	1010	1.8×10^8	0.18	0.28
	PhCN	1180	9.3×10^7	0.11	0.44
	DMF	960	d	d	0.47
2	toluene	1100	c	c	−0.23
	THF	1010	1.8×10^8	0.18	0.32
	PhCN	1150	1.1×10^8	0.13	0.49
	DMF	940	d	d	0.52
4	toluene	1380	c	c	−0.40
	THF	50	1.8×10^{10}	0.96	0.07
	PhCN	1.0	7.3×10^9	0.91	0.22
	DMF	100[e]	9.1×10^9	0.93	0.24

[a] Calculated by the following equations: $k_q^S = \tau_F^{-1} - \tau_0^{-1}$ and $\Phi_q^S = (\tau_F^{-1} - \tau_0^{-1})/\tau_F^{-1}$, where the lifetimes of reference **4** (τ_0) were evaluated to be 1130 ps (toluene), 1230 ps (THF), 1330 ps (PhCN), and 910 ps (DMF), and those of reference **5** were evaluated to be 1300 ps (toluene). [b] ΔG_{CS}^S values were calculated from the Weller equation ($\Delta G_{CS}^S = E_{ox}(TPA) - E_{red}(C_{60}) - E_0 - E_c$),[34] employing the E_S energy level of $^1C_{60}$* (=1.75 eV) and the $E_{red}(C_{60})$ and $E_{ox}(TPA)$ shown in the text. E_c (Coulombic enery) was calculated by $(e^2/(4\pi\epsilon_0))[(1/(2R_+) + 1/(2R_-) - 1/R_{D-R})/\epsilon_S - (1/(2R_+) + 1/(2R_-))/\epsilon_R]$, where R_+, R_-, and R_{D-R} are the radii of the cation and anion and the center-to-center distance between the donor and acceptor, respectively. ϵ_S and ϵ_R are dielectric constants of the solvents used for photophysical studies and for measuring the redox potentials, respectively.[34] [c] No quenching within experimental error. [d] $\tau_F < \tau_0$; the reason is not clear. [e] In DMF fluorescence decay was fitted with biexponential decays, giving 100 ps (81%) and 1300 ps (19%).

the rate constant k_q^S and the quantum yield Φ_q^S for fluorescence quenching were calculated and are summarized in Table 1. The k_q^S values of **1** and **2** are in the range of $(1-2) \times 10^8$ s^{-1}, and the Φ_q^S values are in the range of 0.11−0.20. By comparing the k_q^S and Φ_q^S values with the intersystem-crossing (ISC) rate constant ($k_{ISC} = 8.5 \times 10^8$ s^{-1})[36] and quantum yields ($\Phi_{ISC} = 0.92-0.96$)[36] of **4**, it was shown that the main decay process of the $^1C_{60}$* moiety in **1** and **2** is an ISC, leading to the $^3C_{60}$* moiety even in polar solvents.

From the negative ΔG_{CS}^S values in polar solvents, the CS process via the $^1C_{60}$* moiety in **1** and **2** appears to be thermodynamically favorable; thus, the evaluated k_q^S and Φ_q^S values can be attributed to the CS process via the $^1C_{60}$* moiety in rotaxanes **1** and **2**. However, the CS process via the $^1C_{60}$* moiety is not the main process, since the k_q^S and Φ_q^S values are quite small. This is characteristic of these rotaxanes.

Compared with the rotaxanes, the efficient CS process of the covalently bonded C_{60}−TPA dyad **3** via $^1C_{60}$* was suggested from the rapid decays of fluorescence time profiles in polar solvents as shown in Figure 6b. The time profiles show biexponential decay in DMF, PhCN, and THF; the lifetimes of the C_{60} moieties in **3** were evaluated by the curve-fitting method. The slow decay component (ca. 1.3 ns) exhibited a low contribution (7%) while the fast decay component (130 ps) showed a major contribution (93%) in PhCN (Table 1). Comparing **3** with [2]rotaxanes **1** and **2**, the CS process from **3** is rapid in polar solvents; the k_q^S values are in the range of $(7-20) \times 10^9$ s^{-1}, accounting for Φ_q^S = ca. 0.91−0.96. Thereby, these k_q^S and Φ_q^S values can be thought of as k_{CS}^S and Φ_{CS}; thus, the k_{CS}^S values are larger than k_{ISC} of the C_{60} moiety.[36]

Time-Resolved Transient Absorption Spectra. Figure 7 shows the time-resolved transient absorption spectrum of [2]rotaxane **2** in toluene observed by nanosecond laser photolysis

TABLE 2: CS Rate Constants (k_{CS}^T), CS Minimum Quantum Yields ($\Phi_{CS}^T{}_{min}$), CR Rate Constants (k_{CR}^T), and Lifetimes (τ_{RIP}) of the Radical Ion Pair and Free-Energy Changes ($-\Delta G_{CR}$) of Charge Recombination of [2]Rotaxanes 1 and 2 in THF, PhCN, and DMF

[2]rotaxane	solvent	k_{CS}^T/s^{-1}	$\Phi_{CS}^T{}_{min}$	$-\Delta G_{CS}^T$/eV	k_{CR}/s^{-1}	τ_{RIP}/ns	$-\Delta G_{CR}{}^a$/eV
1	THF	7.3×10^7	0.95	0.03	3.5×10^6	290	1.49
	PhCN	6.0×10^7	0.88	0.19	2.8×10^6	360	1.33
	DMF	8.2×10^7	0.90	0.22	5.9×10^6	170	1.30
2	THF	7.2×10^7	0.96	0.07	3.4×10^6	290	1.45
	PhCN	5.7×10^7	0.97	0.24	3.5×10^6	290	1.28
	DMF	7.9×10^7	0.95	0.27	5.0×10^6	200	1.25

[a] $-\Delta G_{CR} = -E_{ox} + E_{red} - E_c$; see the margin in Table 1.

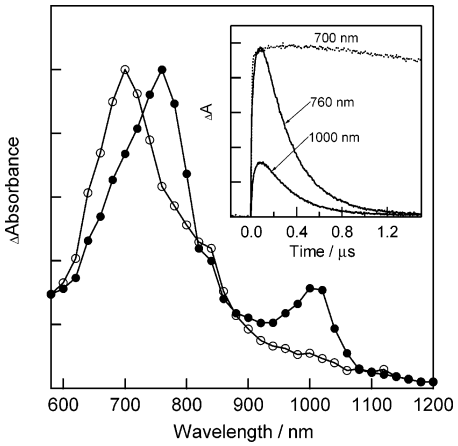

Figure 7. Nanosecond transient absorption spectra of [2]rotaxane **2** (0.1 mM) observed by 532 nm laser irradiation after 100 ns in PhCN (●) and in toluene (○). Inset: Absorption−time profiles at 700 nm in TN and at 760 and 1000 nm in PhCN.

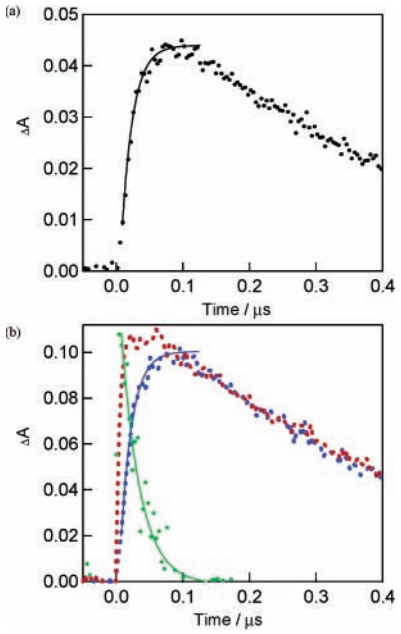

Figure 8. Absorption−time profiles of [2]rotaxane **1** (a) at 1000 nm and (b) at 700 nm (red) and 1000 nm (blue, normalized at time 100 ns) and the profile subtracted from that at 700 nm (green) in PhCN.

with 532 nm laser excitation (6 ns laser pulse) (○). The peak at 700 nm was determined to come from the $^3C_{60}$* moiety in **2**, because a similar absorption was observed for **4** in every solvent under the same conditions. In the transient spectrum of **2** in PhCN (● in Figure 7), on the other hand, transient absorption bands appeared around 760 and 1000 nm. The latter band was attributed to the $C_{60}^{\bullet-}$ moiety. The absorption band in the visible region around 760 nm was assigned to the $TPA^{\bullet+}$ moiety in the rotaxane, although a slight shift from the peak in Figure 3 was observed. Comparing the ratio of the extinction coefficient of the $TPA^{\bullet+}$ moiety at 760 nm to that of the $C_{60}^{\bullet-}$ moiety at 1000 nm, which is ca. 3, leads to the observation that the transient spectrum in PhCN results exclusively from the CS state $(C_{60}^{\bullet-},TPA^{\bullet+})_{rotaxane}$. Similar transient absorption spectra suggesting the formation of $(C_{60}^{\bullet-},TPA^{\bullet+})_{rotaxane}$ were obtained in DMF and THF in both [2]rotaxanes **1** and **2**. It is thus reasonable to assume that the CS state $(C_{60}^{\bullet-},TPA^{\bullet+})_{rotaxane}$ easily acquires the triplet spin character, because the precursor of the CS state is the $^3C_{60}$* moiety in the rotaxanes.

The inset time profile at 700 nm shows the slow decay of the transient species of **2** in toluene, in which the 700 nm band is attributed to the triplet state of the $^3C_{60}$* moiety in **2**. Two curves at 760 and 1000 nm in the inset of Figure 7 show the time profiles of $(C_{60}^{\bullet-},TPA^{\bullet+})_{rotaxane}$ in PhCN corresponding to the decay (100−1200 ns) of the $TPA^{\bullet+}$ and $C_{60}^{\bullet-}$ moieties after reaching maxima at ca. 100 ns. The decays in polar solvents obey first-order kinetics with rate constants in the range of $(2-5) \times 10^6\ s^{-1}$, which are attributed to the CR rate constant (k_{CR}^T) as summarized in Table 2. The small k_{CR}^T values observed suggest that the CR process lies in an inverted region far more negative than the reorganization energy. From the inverse of the k_{CR}^T values, the lifetimes (τ_{RIP}) of the radical ions $(C_{60}^{\bullet-},TPA^{\bullet+})_{rotaxane}$ were evaluated. The longest τ_{RIP} value was 360 ns for rotaxane **1** in PhCN, while the shortest τ_{RIP} value was 170 ns for rotaxane **1** in DMF. It may thus be deduced that there are no distinct difference in τ_{RIP} values between rotaxanes **1** and **2**.

In the time profile at 1000 nm on a shorter time scale than 100 ns, a rise and successive decay in $C_{60}^{\bullet-}$ absorption were observed (Figure 8a). From the curve fitting with a single exponential, the CS rate constants (k_{CS}^T) via the $^3C_{60}$* moiety in the two rotaxanes in polar solvents were calculated; the results are listed in Table 2. The k_{CS}^T values were in the range of $(5-9) \times 10^7\ s^{-1}$.

Figure 8b shows the time profile at 700 nm in PhCN, in which the rapid decay of the absorption of the $^3C_{60}$* moiety and the rise of the $TPA^{\bullet+}$ moiety in rotaxane **2** may be overlapped. On assuming the rise curve for the $TPA^{\bullet+}$ moiety is similar to that of the $C_{60}^{\bullet-}$ moiety at 1000 nm, the observed 700 nm time profile was found to be curve-resolved as shown in Figure 8b: The extracted decay rate of the $^3C_{60}$* moiety ($5.5 \times 10^7\ s^{-1}$) was almost the same as the rise rate ($6.0 \times 10^7\ s^{-1}$), unambiguously confirming that the $C_{60}^{\bullet-}$ moiety and $TPA^{\bullet+}$ moiety are generated via the $^3C_{60}$* moiety.

On the other hand, the transient spectrum of **3** in toluene (Figure 9) is nearly identical to that of the excited triplet state of *N*-methylpyrrolidinofullerene C_{60} ($^3NMPC_{60}$*) (**5**). Therefore, the transient absorption at 700 nm can be attributed to that of the $^3C_{60}$* moiety in **3**. Although **3** still displays the same transient absorption spectrum in PhCN, the absorption intensity of the $^3C_{60}{}^*$ moiety was considerably lower than that in toluene under the same experimental conditions. This lower absorption

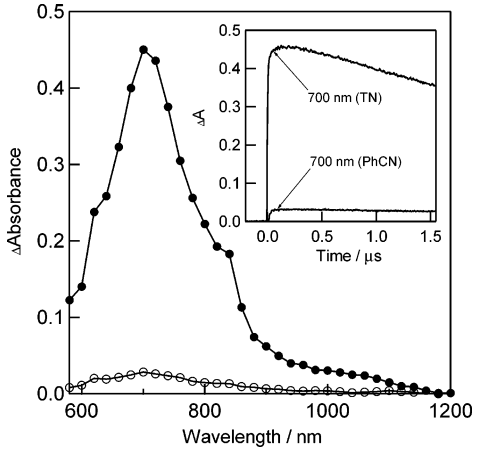

Figure 9. Nanosecond transient absorption spectra of **3** (0.1 mM) observed by 532 nm laser irradiation after 100 ns in toluene (●) and in PhCN (○). Inset: Absorption−time profiles at 700 nm in toluene and PhCN.

in PhCN indicates the presence of a competitive path with ISC via $^1C_{60}{}^*$. However, in DMF and THF, very weak transient absorption bands at 700 nm were detected as compared to that in PhCN. The $\Phi_{CS}{}^S$ values estimated to be 0.91 (PhCN), 0.93 (DMF), and 0.96 (THF) from the τ_f values are in excellent agreement with the low ratio of the generation of $^3C_{60}{}^*$ via ISC. Furthermore, since the absorption of the $C_{60}{}^{\bullet-}$ moiety was minimal in the 1000−1100 nm region even in polar solvents within the laser light pulse (6 ns), it is most likely that an extremely fast CR process takes place immediately after the rapid CS process via $^1C_{60}{}^*$ with the nanosecond laser pulse (6 ns) in the case of the covalent dyad **3**.

When $NMPC_{60}$ (**5**) was photoexcited in the presence of equimolar TPA in PhCN by nanosecond laser light with 532 nm, the observed transient spectra were quite similar to those of the $^3NMPC_{60}$* moiety of **3** (see Supporting Information Figure S1). Immediately following laser excitation, the absorption of $^3NMPC_{60}$* of 700 nm was observed, while the absorption of $NMPC_{60}{}^{\bullet-}$ at 1000 nm was not observed, indicating that intermolecular ET did not appreciably take place in the presence of a low concentration of TPA. With an increase in TPA concentration (up to 50 times more than that of **5**), both the decay rate of $^3NMPC_{60}$* and the rise rate of $NMPC_{60}{}^{\bullet-}$ increased, indicating that intermolecular ET from TPA to $^3NMPC_{60}$* occurred to a certain extent. Under pseudo-first-order conditions, the bimolecular ET rate constant was determined to be in the range of 10^8 M^{-1} s^{-1} in PhCN. From this value, the first-order rate constant for intermolecular ET in the presence of 0.1 mM TPA was calculated to be 10^4 s^{-1}, which is far smaller than the $k_{CS}{}^T$ values for rotaxanes **1** and **2** in PhCN by factors of 1/200 to 1/500.

The quantum yields ($\Phi_{CS}{}^T$) of the formation of the CS state in rotaxanes **1** and **2** via the $^3C_{60}$* moiety were estimated from the ratio of the maximal absorbance at 1000 nm of the $C_{60}{}^{\bullet-}$ moiety to the initial absorbance at 700 nm of the $^3C_{60}$* moiety by substituting each molar extinction coefficient,[36] assuming that the initial absorbance at 700 nm is predominantly attributed to the $^3C_{60}$* moiety as shown in Figure 8. If the initial absorbance of the $^3C_{60}$ moiety at 700 nm contains the absorption of $TPA^{\bullet+}$ moieties, the $\Phi_{CS}{}^T$ values calculated by this method can be regarded as minimum values of $\Phi_{CS}{}^T$ ($\Phi_{CS}{}^T{}_{min}$). Such $\Phi_{CS}{}^T{}_{min}$ values are in the range of 0.88−0.97, as summarized in Table 2. If these values are compared with the $\Phi_{CS}{}^S$ of less than 0.2 for rotaxanes **1** and **2**, it can be assumed that the CS takes place mainly from $^3C_{60}$* in [2]rotaxanes **1** and **2**, resulting in the formation of $(C_{60}{}^{\bullet-},TPA^{\bullet+})_{rotaxane}$. These findings indicate that the $^3C_{60}$* moiety in the rotaxanes, which is formed predominantly via the $^1C_{60}$* moiety with ISC, induces an intrarotaxane CS with high $\Phi_{CS}{}^T$ values.

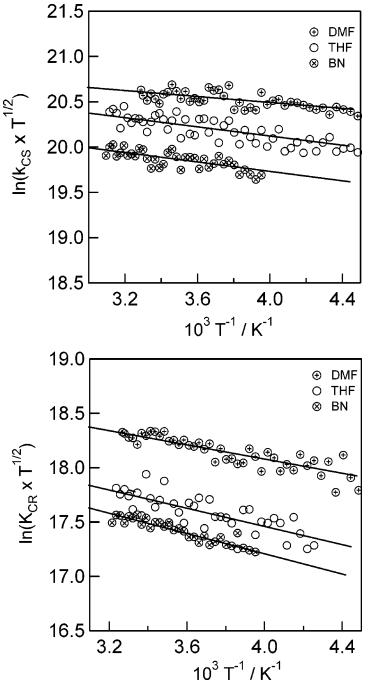

Figure 10. Modified Arrhenius plots of the temperature-dependent $k_{CS}{}^T$ and k_{CR} for [2]rotaxane **1** in DMF, PhCN, and THF.

TABLE 3: Activation Energies and Reorganization Energies for [2]Rotaxanes 1 and 2 in DMF, BN, and THF

[2]rotaxane	solvent	$-\Delta G^{\ddagger}_{CS}{}^T$/eV	$\lambda_{CS}{}^T$/eV	$-\Delta G^{\ddagger}_{CR}$/eV	λ_{CR}/eV
1	THF	0.026	0.006	0.036	0.14
	PhCN	0.015	0.11	0.039	0.15
	DMF	0.017	0.13	0.028	0.11
2	THF	0.019	0.026	0.058	0.23
	PhCN	0.021	0.13	0.040	0.16
	DMF	0.014	0.17	0.031	0.12

Temperature Effect. The $k_{CS}{}^T$ and k_{CR} of [2]rotaxanes **1** and **2** were of slight temperature dependence; in DMF, PhCN, and THF, the $k_{CS}{}^T$ and k_{CR} values decreased with a decrease in temperature in each solvent. For example, the k_{CR} values decreased from 5.3×10^6 s^{-1} at 35 °C to 3.8×10^6 s^{-1} at −38 °C in DMF. Although the difference between the rate constants was small, such a small difference is larger than the experimental errors included in our experiments. From a semiclassical Marcus equation,[38] the ET rate constant (k_{ET}) can be described as shown in eq 1,

$$\ln(k_{ET}T^{1/2}) = \ln\{2\pi^{3/2}|V|^2/[h(\lambda k_B)^{1/2}]\} - \Delta G^{\ddagger}/(k_B T) \quad (1)$$

where T, h, k_B, $|V|$, λ, and $\Delta G^{\ddagger T}$ are referred to as the absolute temperature, Planck constant, Boltzmann constant, electron coupling matrix element, reorganization energy, and Gibbs activation energy in Marcus theory. The plots of $\ln(k_{CS}{}^T T^{1/2})$ and $\ln(k_{CR}{}^T T^{1/2})$ vs $1/T$ for rotaxane **1** are shown in parts a and b, respectively, of Figure 10. Similar figures were obtained for rotaxane **2**. Since the slopes were not steep in any case, the $\Delta G^{\ddagger}_{CS}{}^T$ and $\Delta G^{\ddagger}_{CR}$ values below 0.026 and 0.050 eV were, respectively, evaluated, as summarized in Table 3. The $\Delta G^{\ddagger}_{CR}{}^T$ values in rotaxanes were found to be much smaller than those in conventional dyad systems such as retinyl−C_{60} (0.16 eV) and diphenylamine-substituted fullerene C_{60} (0.11 eV) dyads.[39]

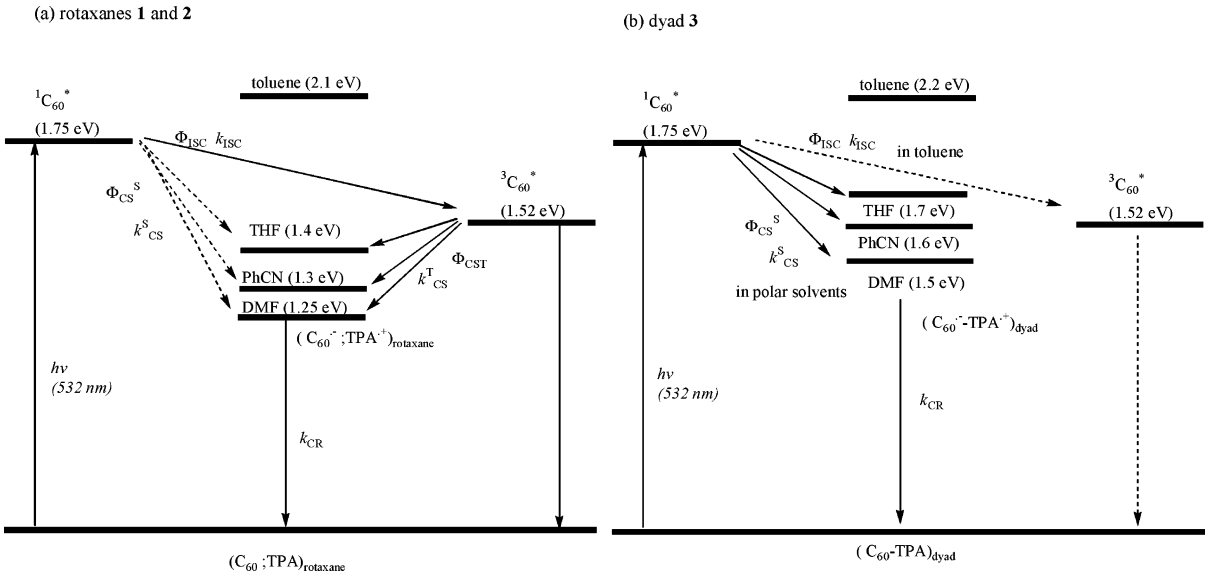

Figure 11. Energy diagrams and flows of excitation energy and electrons: (a) [2]rotaxanes **1** and **2**, (b) dyad **3**.

$\Delta G^{\ddagger}_{CS}{}^{T}$ values below 0.026 eV imply that the CS process occurs under nearly optimal conditions without any barrier on the basis of the Marcus theory.[38] The λ values can be evaluated from eq 2,

$$\Delta G^{\ddagger}_{ET} = (\Delta G^{\circ} + \lambda)^2/4\lambda \qquad (2)$$

where ΔG° is referred to as ΔG°_{CS} and ΔG°_{CR}. The λ values summarized in Table 3 are also considerably smaller than $\Delta G^{\circ}_{CS}{}^{T}$ and ΔG°_{CR}, indicating that the CS and CR rates are in the inverted region of the Marcus parabola.[38] Thus, the observed small $k_{CS}{}^{T}$ and k_{CR} values on the order of 10^7 and 10^6 s^{-1}, respectively, are reasonably interpreted. The $|V|$ values for **1** and **2** in three kinds of solvents are extremely small compared with the reported V values ($1-100$ cm^{-1}) for covalently bonded dyad systems.[40,41] The considerably smaller λ and $|V|$ values in rotaxanes **1** and **2** may be explained by the fact that the CS and CR processes are governed mainly by pure "through-space" electronic coupling between C_{60} and TPA moieties and that there is little contribution for "through-bond" electronic coupling. The λ value may thus be minimized because the chemical bond rearrangements associated with the CS and CR processes in **1** and **2** would be negligibly small, resulting in the drop out of the internal reorganization energy, leaving only the reorganization energy for the solvents. Furthermore, it is concluded that the λ values for the CS via $^1C_{60}{}^*$ in rotaxanes **1** and **2** are small, resulting in low $k_{CS}{}^{S}$ compared to k_{ISC} for CS via $^1C_{60}{}^*$. As for the small $|V|$, it should be noted that there is little difference between **1** and **2**. This is because electronic coupling between the C_{60} and TPA moieties occurs through space without the help of the weak hydrogen bond of the ammonium group to the crown ether ring in **1**. Conversely, this evidence strongly supports the existence of pure through-space CS and CR processes in **1** and **2**.

Energy Diagrams. From the ΔG_{CR}, $\Delta G_{CS}{}^{S}$, and $\Delta G_{CS}{}^{T}$ data as well as the energy levels of the lowest excited singlet states, the energy diagrams for rotaxanes **1** and **2** and the covalently bonded dyad **3** may be drawn, as shown in Figure 11. In less polar solvents such as toluene, since the energy levels of the CS state of **1** and **2** are higher than those of both $^1C_{60}$* and $^3C_{60}$*, no CS process was observed; thus, $^3C_{60}$* was only observable with a long lifetime of over 20 μs. In polar solvents such as DMF, PhCN, and THF, since the energy levels of the CS state of **1** and **2** were lower than those of both $^1C_{60}$* and $^3C_{60}$*, the CS processes via both $^1C_{60}$* and $^3C_{60}$* are possible. Since the observed $\Phi_{CS}{}^{S}$ values of **1** and **2** were smaller than Φ_{ISC}, most of $^1C_{60}$* was converted to $^3C_{60}$*, from which the CS takes place with high $\Phi_{CS}{}^{T}$. Thus, the rotaxanes can be said to involve both the minor CS process via $^1C_{60}$* and the major CS process via $^3C_{60}$*, resulting in the generation of CS states with lifetimes of several hundred nanoseconds, because of the small λ values which are lower than ΔG°_{CR} as well as because of the triplet character of the CS states in the rotaxanes.

On the other hand, in the covalently bonded $^1C_{60}$*−TPA dyad **3**, the energy levels of the CS states in polar solvents are lower than in the $^1C_{60}$* moiety, resulting in large $k_{CS}{}^{S}$ values with high $\Phi_{CS}{}^{S}$ values. Although the Marcus parameters were not obtained for **3**, the small $\Delta G_{CS}{}^{S}$ values obtained suggest that the CS process is far below the top region of the Marcus parabola in the normal region.[38] Therefore, the relatively large $k_{CS}{}^{S}$ values with high $\Phi_{CS}{}^{S}$ values may be caused by a large electron-coupling matrix element for this dyad, suggesting that the CS process via $^1C_{60}$* mainly takes place through bond, which also explains the through-bond fast CR process of **3**.

Difference between Rotaxanes 1 and 2 and Solvent Effects. In each polar solvent, rotaxanes **1** and **2** had very similar $k_{CS}{}^{T}$ values; however, the $\Phi_{CS}{}^{T}$ values for rotaxane **2** tended to be slightly higher than those for rotaxane **1**. In terms of k_{CR} values, no clear difference between rotaxanes **1** and **2** was found. Although a rather strong interaction between the axle and the crown ether in rotaxane **1** is indicative of faster rates than those of rotaxane **2**, the longer R_{cc} values than that of rotaxane **1** may compensate the interaction between the C_{60} and TPA moieties. The shorter R_{cc} of rotaxane **2** may trigger higher $\Phi_{CS}{}^{T}$ values.

In each rotaxane **1** and **2**, the order of $k_{CS}{}^{T}$ is PhCN < THF < DMF; the k_{CR} values also show a similar order. This type of solvent dependency may be in part explained by the difference in stabilization ability for the charged species as shown by ΔG_{CR}. But, in general, the Lewis base character also affects the flexibility or the mobility of the components of rotaxane, especially of a rotaxane bearing intramolecular hydrogen bonding such as **1**.[31,37] Therefore, solvent effects on rate parameters are governed by both polarity and Lewis acidity.

Comparison with Other Dyads, Pseudorotaxane, and Rotaxane. [2]Rotaxanes **1** and **2** have τ_{RIP} values similar to that of a different type of rotaxane bearing C_{60} and porphyrin,

which has a τ_{RIP} value of 180 ns in PhCN at room temperature, as recently reported,[18] despite some CS mechanistic differences between them. In the rotaxane with C_{60} and porpyrin, the CS process mainly proceeds via the singlet excited state of the porphyrin moiety.[18] Meanwhile, for the pseudorotaxane with C_{60} and phthalocyanine, a τ_{RIP} value of 1500 ns was reported in PhCN at room temperature.[17] These τ_{RIP} values for rotaxanes seem to be longer than those of corresponding covalently bonded dyads. One example is shown for the C_{60}−TPA dyad in the present study. Covalently linked C_{60}−dimethylaniline dyads are also reported to have shorter τ_{RIP} values than those of rotaxanes.[19a]

In the case of rotaxanes composed of zinc porphyrin as electron donor and Au^{+} porphyrins as electron acceptor, the existence of a superexchange mechanism was confirmed.[42] However, for [2]rotaxanes **1** and **2**, no clear evidence of a superexchange mechanism was obtained, probably because of the smaller π-system of the TPA moiety.

Conclusions

In C_{60}/TPA-containing rotaxanes, a photoinduced CS process taking place mainly via the $^3C_{60}$* moiety, producing a long-lived CS state $(C_{60}^{\bullet-},TPA^{\bullet+})_{rotaxane}$, was observed in a polar solvent. However, in a covalently bonded C_{60}−TPA dyad system, the lifetime of the CS state was found to be short, although the rates of the fastest CS processes ranged between 7×10^9 and 20×10^9 s^{-1} in polar solvents. For the rotaxanes (C_{60},TPA), through-space CS and CR processes were presumed from the low activation free energies, small reorganization energy, and small electron coupling matrix elements as evaluated experimentally by temperature dependence of the rate constants. It was shown that efficient CS takes place via $^3C_{60}$* with a high quantum yield in rotaxanes (C_{60},TPA), in contrast to covalently bonded C_{60}−TPA dyads, in which efficient CS takes place via $^1C_{60}$* with a quick CR process.

Experimental Section

General Procedures. Melting points were measured on a Yanagimoto micro melting point apparatus and were uncorrected. IR spectra were recorded on a JASCO FT-IR model 230 spectrometer. ^{1}H and ^{13}C NMR measurements were performed on JEOL JNM-GX-270 and JNM-L-400 spectrometers in $CDCl_3$ with tetramethylsilane as an internal reference. FAB-MS measurements were performed on a Finnigan TSQ-70 instrument. Steady-state absorption spectra in the visible and near-IR regions were measured on a Jasco V570 DS spectrometer. Fluorescence spectra were measured on a Shimadzu RF-5300PC spectrofluorophotometer.

For preparative HPLC, a JAICO LC-908 system using columns JAIGEL 1 (∅ 20 mm × 600 mm) and JAIGEL 2 (∅ 20 mm × 600 mm) was employed. Compounds **7**, **9**, and **11** were prepared according to methods described previously.[26−29] [60]Fullerene was purchased from Frontier Carbon Corp. Other materials of reagent grade were used without further purification.

Synthesis of Bis(bromomethyl) Crown Ether 8. To a solution of paraformaldehyde (92%, 327 mg, 10 mmol) and **7** (2.1 g, 4.0 mmol) in acetic acid (10 mL)/$CHCl_3$ (10 mL) was added 40% HBr in acetic acid (5.0 mL). After being stirred for 40 h at 45 °C, the reaction mixture was poured into cold water and extracted with $CHCl_3$. The extract was washed successively with water and brine, dried over anhydrous $MgSO_4$, and evaporated to dryness. The residue was subjected to silica gel column chromatography (eluent $CHCl_3$/methanol (95/5)) to afford **8** as a white solid (1.32 g, 47%): mp 152−154 °C; ^{1}H NMR (400 MHz, $CDCl_3$) δ 7.65 (dd, 1H, J = 2.1, 6.4 Hz), 7.52 (d, 1H, J = 2.0 Hz), 6.84 (d, 1H, J = 8.3 Hz), 6.82 (s, 2H), 4.59 (s, 4H), 4.34 (q, 2H, J = 6.8 Hz), 4.31−4.15 (m, 8H), 3.95−3.82 (m, 16H), 1.38 (t, 3H, J = 7.3 Hz) ppm; IR (NaCl) 2877, 1715, 1603, 1523, 1431, 1362, 1276, 1220, 1195, 1132, 1057, 993, 871, 760 cm^{-1}; FAB-MS (matrix mNBA) m/z = 706 $[M + H]^+$.

Synthesis of Crown Ether 4. A mixture of C_{60} (468 mg, 0.7 mmol), **8** (353 mg, 0.5 mmol), 18-crown-6 (528 mg, 2.0 mmol), and KI (498 mg, 3.0 mmol) was refluxed in dry toluene for 36 h in the dark. The reaction mixture was directly subjected to SiO_2 column chromatography (eluent toluene to $CHCl_3$/methanol (95/5)) to collect a dark brown band, which was further purified by preparative GPC (eluent $CHCl_3$) to give **4** as a dark brown solid (254 mg, 40%): mp 142−144 °C; ^{1}H NMR (400 MHz, $CDCl_3$) δ 7.65 (dd, 1H, J = 2.0, 8.3 Hz), 7.54 (d, 1H, J = 2.0 Hz), 7.20 (s, 2H), 6.86 (d, 1H, J = 2.0 Hz), 4.71−4.70 (m, 2H), 4.37−4.22 (m, 12H), 4.02−3.90 (m, 16H), 1.38 (t, 3H, J = 7.1 Hz) ppm; ^{13}C NMR (67.5 MHz, $CDCl_3$) δ 166.24, 156.87, 156.60, 152.61, 148.34, 148.06, 147.55, 146.36, 146.11, 145.70, 145.33, 144.60, 143.01, 142.45, 142.15, 141.96, 141.49, 140.00, 136.04, 135.40, 130.60, 123.75, 123.10, 114.05, 113.75, 111.77, 77.47, 71.46, 71.46, 69.98, 69.71, 69.58, 69.37, 69.20, 66.02, 60.73, 44.69, 14.36 ppm; IR (NaCl) 2925, 1717, 1653, 1602, 1559, 1507, 1457, 1271, 1215, 1108, 955, 843, 752 cm^{-1}; FAB-MS (matrix mNBA) m/z = 1266 $[M + H]^+$. Anal. Calcd for $C_{89}H_{38}O_{10}\cdot(CHCl_3)_{0.75}$: C, 79.45; H, 2.88. Found: C, 79.68; H, 2.84.

Synthesis of [2]Rotaxane 1. To a solution of axle **9** (42 mg, 0.10 mmol) and crown ether **4** (152 mg, 0.12 mmol) in $CHCl_3$ (0.30 mL) was added in the dark a solution of isocyanate **10** (43 mg, 0.15 mmol) in $CHCl_3$ (0.30 mL). After dibutyltin dilaurate (6.3 mg, 0.010 mmol) was added, the mixture was stirred at room temperature for 20 h and evaporated to dryness. The residue was subjected to preparative GPC (eluent $CHCl_3$) to afford [2]rotaxane **1** as a dark brown solid (150 mg, 76%): ^{1}H NMR (400 MHz, $CDCl_3$, 333 K) δ 7.65 (d, 1H, J = 8.3 Hz), 7.52 (s, 1H), 7.37−7.14 (m, 12H), 7.01−6.89 (m, 11H), 4.74 (br, 2H), 4.46 (br, 4H), 4.33−4.21 (m, 8H), 4.02−3.73 (m, 16H), 3.53 (br, 6H), 1.98 (br, 2H), 1.36−1.31 (m, 3H), 1.24 (s, 18H) ppm; IR (NaCl) 3391, 2961, 1715, 1589, 1511, 1269, 1208, 1106, 954, 844 752 cm^{-1}; FAB-MS (matrix mNBA) m/z = 1831 $[M - PF_6]^+$. Anal. Calcd for $C_{126}H_{84}F_6N_3O_{12}P\cdot(CHCl_3)_{1.0}$: C, 72.76; H, 4.09; N, 2.00. Found: C, 72.91; H, 4.46; N, 2.23.

Synthesis of [2]Rotaxane 2. To a solution of **1** (59 mg, 0.03 mmol) in CH_3CN (0.40 mL) were added acetic anhydride (8.5 μL, 0.09 mmol) and triethylamine (13.8 μL, 0.10 mmol) in the dark. The mixture was stirred at room temperature for 3 h, during which a black precipitate was formed. The precipitate was dissolved by the addition of $CHCl_3$ (0.10 mL), and stirred at room temperature for 25 h. A black precipitate was once again formed. The reaction mixture was filtered off, and the precipitate was washed with CH_3CN and then MeOH. The residue was dissolved in $CHCl_3$ and then subjected to preparative GPC (eluent $CHCl_3$) to afford [2]rotaxane **2** as a dark brown solid (49 mg, 89%): mp 157−160 °C; ^{1}H NMR (400 MHz, $CDCl_3$, 333 K) δ 8.57 (s, 0.5H), 8.41 (s, 0.5H), 7.61−7.46 (m, 4H), 7.31−7.24 (m, 2H), 7.13 (br, 5H), 6.96−6.88 (m, 10H), 6.77−6.76 (m, 1H), 4.46−4.21 (m, 18H), 3.81 (br, 8H), 3.51−3.32 (m, 10H), 1.97 (s, 3H), 1.92 (br, 2H), 1.39−1.35 (m, 3H), 1.29 (s, 18H) ppm; IR (NaCl) 2961, 1716, 1636, 1598, 1508, 1268, 1216, 1113 cm^{-1}; FAB-MS (matrix mNBA) m/z = 1871 $[M + H]^+$. Anal. Calcd for $C_{128}H_{85}N_3O_{13}\cdot(CHCl_3)_{1.0}$: C, 77.76; H, 4.35; N, 2.11. Found: C, 77.98; H, 4.68; N, 2.28.

Synthesis of *N*-Boc Axle 12. To a solution of **11** (378 mg, 1.00 mmol) and isocyanate **10** (387 mg, 1.35 mmol) in $CHCl_3$ (25 mL) was added dibutyltin dilaurate (60 μL, 0.10 mmol). The mixture was stirred at room temperature for 24 h and then evaporated to dryness. The residue was subjected to preparative GPC (eluent $CHCl_3$) to afford **12** as an off-white solid (398 mg, 60%): ^{1}H NMR (270 MHz, $CDCl_3$, 323 K) δ 7.30−7.17 (m, 7H), 7.04−6.93 (m, 10H), 6.47 (br, 1H), 4.42 (s, 2H), 4.14 (t, 2H, J = 6.3 Hz), 3.31 (br, 2H), 1.92−1.82 (m, 2H), 1.47 (s, 9H, O^{t}Bu), 1.30 (s, 18H) ppm; IR (NaCl) 3314, 2963, 1696, 1592, 1513, 1494, 1416, 1273, 1219, 1170, 1061 cm^{-1}.

Synthesis of Axle 6. To a solution of **12** (332 mg, 0.50 mmol) in $CHCl_3$ (3.0 mL) was added trifluoroacetic acid (3.0 mL), and the mixture was stirred at room temperature for 1 h. The reaction mixture was evaporated, and the residue was dissolved in $CHCl_3$. The solution was washed with 10% aqueous K_2CO_3, 5% aqueous HPF_6, water, and then brine, dried over anhydrous $MgSO_4$, filtered, and evaporated to dryness to afford axle **6** as a gray solid (284 mg, 80%): mp 83−86 °C; ^{1}H NMR (270 MHz, CD_3CN, 323 K) δ 7.80 (br, 1H), 7.52 (d, 1H, J = 1.6 Hz), 7.36−7.23 (m, 8H), 7.03−6.98 (m, 8H), 4.21 (t, 2H, J = 6.0 Hz), 4.16 (s, 2H), 3.16 (t, 2H, J = 6.8 Hz), 2.11−2.02 (m, 2H), 1.31 (s, 18H) ppm; IR (NaCl) 2964, 1698, 1593, 1523, 1493, 1273, 1228, 1075, 847, 558 cm^{-1}; FAB-MS (matrix mNBA) m/z = 564 [M − PF_6]$^+$. Anal. Calcd for $C_{37}H_{46}F_6N_3O_2P$: C, 62.61; H, 6.53; N, 5.92. Found: C, 62.85; H, 6.73; N, 5.98.

Spectral Measurements. The time-resolved fluorescence spectra were measured by the single-photon-counting method using the second harmonic generation (SHG; 410 nm) of a Ti:sapphire laser [Spectra Physics, Tsunami 3950-L2S, 1.5 ps full width at half-maximum (fwhm)] and a streak scope (Hamamatsu Photonics, C4334-01) equipped with a polychromator (Action Reasearch, SpectraPro 150) as excitation source and detector, respectively.

Nanosecond transient absorption measurements were carried out using the SHG (532 nm) of a Nd:YAG laser (Spectra Physics, Quanta-Ray GCR-130, fwhm 6 ns) as excitation source. For the transient absorption spectra in the near-IR region (600−1600 nm), the monitoring light from a pulsed Xe lamp was detected with a Ge-avalanche photodiode (Hamamatsu Photonics, B2834). The photoinduced events in the micro- and millisecond time regions were estimated using a continuous Xe lamp (150 W) and an InGaAs−PIN photodiode (Hamamatsu Photonics, G5125-10) as probe light and detector, respectively. The details of the transient absorption measurements were described elsewhere.[34] All the samples in a quartz cell (1 × 1 cm) were deaerated by bubbling argon through the solution for 15 min.

Electrochemical Measurements. The cyclic voltammetry measurements were performed on a BAS CV-50 W electrochemical analyzer in deaerated PhCN solution containing 0.10 M Bu_4NPF_6 as a supporting electrolyte at 298 K (100 mV s^{-1}). The glassy carbon working electrode was polished with BAS polishing alumina suspension and rinsed with acetone before use. The counter electrode was a platinum wire. The measured potentials were recorded using a Ag/AgCl (saturated KCl) electrode as reference electrode.

Acknowledgment. The present work was partly supported by a Grant-in-Aid for Scientific Research on Priority Areas (417) from the Ministry of Education, Science, Sports and Culture of Japan. We are also grateful for the financial support extended by the Core Research for Evolutional Science and Technology (CREST) of the Japan Science and Technology Corp.

Supporting Information Available: Spectroscopic data for compounds **1**, **2**, **4**, and **6** and nanosecond transient spectra of equimolar C_{60} and TPA in PhCN (PDF). This material is available free of charge via the Internet at http//pubs.acs.org.

References and Notes

(1) Ramamurthy, V.; Schanze, K. S. *Molecular and Supramolecular Photochemistry*; Marcel Dekker: New York, 2001; Vol. 7.

(2) Kadish, K. M.; Ruoff, R. S. *Fullerenes*; John Wiley & Sons: New York, 2000; p 225.

(3) (a) Sun, D.; Tham, F. S.; Reed, C. A.; Chaker, L.; Boyd, P. D. W. *J. Am. Chem. Soc.* **2002**, *124*, 6604−6612. (b) Constable, E. C. *Angew. Chem., Int. Ed. Engl.* **1994**, *33*, 2269−2271. (c) Diederich, F.; Gómez-López, M. *Chem. Soc. Rev.* **1999**, *28*, 263−277.

(4) Gust, D.; Moore, T. A.; Moore, A. L. *Acc. Chem. Rec.* **1993**, *26*, 198−205.

(5) Sacriftci, N. S.; Smilowitz, L.; Heeger, A. J.; Wudl, F. *Science* **1992**, *258*, 1474−1476.

(6) (a) Ballardini, R.; Balzani, V.; Clemente-León, M.; Credi, A.; Gandolfi, M. T.; Ishow, E.; Perkins, J.; Stoddart, J. F.; Tseng, H. R.; Wenger, S. *J. Am. Chem. Soc.* **2002**, *124*, 12786−12795 and references therein. (b) Ballardini, R.; Gandolfi, M. T.; Balzani, V. *Electron Transfer in Chemistry*; Wiley-VCH: Weinheim, Germany, 2001; Vol. 3, Chapter 7, pp 539−581. (c) Armaroli, N.; Chambron, J.-C.; Collin, J.-P.; Dietrich-Buchecker, C.; Flamigni, L.; Kern, J.-M.; Sauvage, J.-P. *Electron Transfer in Chemistry*; Wiley-VCH: Weinheim, Germany, 2001; Vol. 3, Chapter 8, pp 582−654.

(7) Williams, R. M.; Koeberg, M.; Lawson, J. M.; Yi-Zhong, A.; Rubin, Y.; Paddon-Row, M. N.; Verhoeven, J. W. *J. Org. Chem.* **1996**, *61*, 5055−5062.

(8) Guldi, D. M.; Maggini, M.; Scorrano, G.; Prato, M. *J. Am. Chem. Soc.* **1997**, *119*, 974−980.

(9) Gust, D.; Moore, T. A.; Moore, A. L. *Res. Chem. Intermed.* **1997**, *23*, 621−651.

(10) (a) Imahori, H.; Yamada, K.; Hasegawa, M.; Taniguchi, S.; Okada, T.; Sakata, Y. *Angew. Chem., Int. Ed. Engl.* **1997**, *36*, 2626−2629. (b) Imahori, H.; Tamaki, K.; Guldi, D. M.; Luo, C.; Fujitsuka, M.; Ito, O.; Sakata, Y.; Fukuzumi, S. *J. Am. Chem. Soc.* **2001**, *123*, 2607−2617. (c) Imahori, H.; Mori, Y.; Matano, J. *J. Photochem. Photobiol., C* **2003**, *4*, 51−83.

(11) Bell, T. D. M.; Smith, T. A.; Ghiggino, K. P.; Ranasinghe, M. G.; Shephard, M. J.; Paddon-Row: M. N. *Chem. Phys. Lett.* **1997**, *268*, 223−228.

(12) Da Ros, T.; Prato, M.; Guldi, D. M.; Alessio, E.; Ruzzi, M.; Pasimeni, L. *Chem. Commun.* **1999**, 635−636. (b) Da Ros, T.; Prato, M.; Guldi, D. M.; Ruzzi, M.; Pasimeni, L. *Chem.—Eur. J.* **2001**, *7*, 816−827. (c) (17) Guldi, D. M.; Luo, C.; Da Ros, T.; Prato, M.; Dietel, E.; Hirsch, A. *Chem. Commun.* **2000**, 375−376. (d) Guldi, D. M.; Luo, C.; Swartz, A.; Scheloske, M.; Hirsch, A. *Chem. Commun.* **2001**, 1066−1067.

(13) Wilson, S. R.; MacMahon, S.; Tat, F. T.; Jarowski, P. D.; Schuster, D. I. *Chem. Commun.* **2003**, 226−227

(14) Diederich, F.; Lopez, M. G. *Chem. Soc. Rev.* **1999**, *28*, 263−277.

(15) Piotrowiak, P. *Chem. Soc. Rev.* **1999**, *28*, 143−150.

(16) (a) D'Souza, F.; Deviprasad, G. D.; El-Khouly, M. E.; Fujitsuka, M.; Ito, O. *J. Am. Chem. Soc.* **2001**, 123, 5277−5284. (b) D'Souza, F.; Deviprasad, G. R.; Zandler, M. E.; Hoang, V. T.; Arkady, K.; Van Stipdonk, M.; Perera, A.; El-Khouly, M. E.; Fujitsuka, M.; Ito, O. *J. Phys. Chem. A* **2002**, *106*, 3243−3243. (c) D'Souza, F.; Deviprasad, G. R.; Zandler, M. E.; El-Khouly, M. E.; Fujitsuka, M.; Ito, O. *J. Phys. Chem. B* **2002**, 106, 4952−4962.

(17) Guldi, D. M.; Ramey, J.; Martinez-Diaz, M. V.; de la Escosura, A.; Torres, T.; Da Ros, T.; Prato, M. *Chem. Commun.* **2002**, 2774−2775.

(18) Watanabe, N.; Kihara, N.; Furusho, Y.; Takata, T.; Araki, Y.; Ito, O. *Angew. Chem., Int. Ed.* **2003**, *42*, 681−683.

(19) (a) Williams, R. M.; Zwier, J. M.; Verhoeven, J. W. *J. Am. Chem. Soc.* **1995**, *117*, 4093−4099. (b) Williams, R. M.; Koeberg, M.; Lawson, J. M.; An, Y.-Z.; Rubin, Y.; Paddon-Row, M. N.; Verhoeven, J. M. *J. Org. Chem.* **1996**, *61*, 5055−5062.

(20) (a) Komamine, S.; Fujitsuka, M.; Ito, O.; Moriwaki, K.; Miyata, T.; Ohno, T. *J. Phys. Chem. A* **2000**, *104*, 11497. (b) Luo, H.; Fujitsuka, M.; Araki, Y.; Ito, O.; Padmawar, P.; Chiang, L. Y. *J. Phys. Chem. B* **2003**, *107*, 9312−9318.

(21) Lawson, G. E.; Kitaygorodskiy, A.; Ya-Ping, S. *J. Org. Chem.* **1999**, *64*, 5913−5920.

(22) (a) Arbogast, J. W.; Foote, C. S.; Kao, M. *J. Am. Chem. Soc.* **1992**, *114*, 2277−2279. (b) Biczok, L.; Linschitz, H. *Chem. Phys. Lett.* **1992**, *195*, 339−346. (c) Nonell, S.; Arbogast, J. W.; Foote, C. S. *J. Phys. Chem.* **1992**, *96*, 4169−4170. (d) Steren, C. A.; von Willigen, H.; Biczok, L.; Gupta, N.; Linschitz, H. *J. Phys. Chem.* **1996**, *100*, 8920.

(23) (a) Ito, O.; Sasaki, Y.; Yoshikawa, Y.; Watanabe. A. *J. Phys. Chem*. **1995**, 99, 9838−9842. (b) Ito, O. *Res. Chem. Intermed*. **1997**, *23*, 389−402. (c) Yahata, Y.; Sasaki, Y.; Fujitsuka, M.; Ito, O. *J. Photosci*. **1999**, *6*, 117−121.

(24) Ghosh, H. N.; Palit, D. K.; Sapre, A. V.; Mittal, J. P. *Chem. Phys. Lett.* **1997**, *265*, 365−373.

(25) Senior, R. J.; Szarka, A. Z.; Smith, G. R.; Hochstrasser, R. M. *Chem. Phys. Lett*. **1991**, *185*, 179−183.

(26) Furusho, Y.; Sasabe, H.; Natsui, D.; Murakawa, K.; Takata, T.; Harada, T. *Bull. Chem. Soc. Jpn*. **2004**, *77*, 179−185.

(27) (a) Diederich, F.; Jonas, U.; Gramlich, V.; Herrmann, A.; Ringsdorf, H.; Thilgen, C. *Helv. Chim. Acta* **1993**, *76*, 2445−2453. (b) Luboch, E.; Cygan, A.; Biernat; J. F. *Tetrahedron* **1990**, *46*, 2461−2472.

(28) Diederich, F.; Echegoyen, L.; Gómez-López, M.; Kessinger, R.; Stoddart, J. F. *J. Chem. Soc., Perkin Trans. 2* **1999**, 1577−1586.

(29) Belik, P.; Gügel, A.; Spickermann, J.; Müllen, K. *Angew. Chem., Int. Ed. Engl*. **1993**, *32*, 78−80.

(30) Kawasaki, H.; Kihara, N.; Takata, T. *Chem. Lett*. **1999**, 1015−1016.

(31) Kihara, N.; Tachibana, Y.; Kawasaki, H.; Takata, T. *Chem. Lett*. **2000**, 506−507.

(32) Takata, T.; Kawasaki, H.; Kihara, N.; Furusho, Y. *Macromolecules* **2001**, *34*, 5449−5456.

(33) Kemp, T. J.; Martins, L. J. A. *J. Chem. Soc., Faraday Trans.* **1981**, *177*, 1425−1435.

(34) Weller, A. *Z. Phys. Chem. Neue Folge* **1982**, *133*, 93−98.

(35) Luo, C.; Fujitsuka, M.; Watanabe, A.; Ito, O.; Gan, L.; Huang, Y.; Huang, C.-H. *J. Chem. Soc., Faraday Trans*. **1998**, *94*, 527−532.

(36) (a) Sension, R. J.; Phillips, C. M.; Szarka, A. Z.; Romanow, W. J.; McGhie, A. R.; McCauly, Jr., J. P.; Smith, A. B., III; Hochstrasser, R. M. *J. Phys. Chem*. **1991**, *95*, 6075−6078. (b) Ebbesen, T. W.; Tanigaki, K.; Kuroshima, S. *Chem. Phys. Lett.* **1991**, *181*, 501−504. (c) Lee, M.; Song, O.-K.; Seo, J.-C.; Kim, D.; Suh, Y. D.; Jin, S. M.; Kim, S. K. *Chem. Phys. Lett*. **1992**, *196*, 325−329. (d) Watanabe, A.; Ito, O.; Watanabe, M.; Saito, H.; Koishi, M. *J. Chem. Soc., Chem. Commun.* **1996**, 117−118.

(37) (a) Ashton, P. R.; Baxter, I.; Fyfe, M. C. T.; Raymo, F. M.; Spencer, N.; Stoddart, J. F.; White, A. J. P.; Williams, J. D. *J. Am. Chem. Soc*. **1988**, *120*, 2297−2307. (b) Tachibana, Y.; Kawasaki, H.; Kihara, N.; Takata, T. Submitted for publication.

(38) (a) Marcus, R. A. *J. Chem. Phys*. **1956**, *24*, 966−978. (b) Marcus, R. A. *J. Chem. Phys.* **1965**, *43*, 679−701. (c) Marcus, R. A.; Sutin, N. *Biochim. Biophys. Acta* **1985**, *811*, 265−322.

(39) (a) Yamazaki, M.; Araki, Y.; Fujitsuka, M.; Ito, O. *J. Phys. Chem. A* **2001**, *105*, 8615−8622. (b) Luo, H.; Fujitsuka, M.; Araki, Y.; Ito, O.; Padmawar, P.; Chiang, L. Y. *J. Phys. Chem. B* **2003**,*107*, 9312−9318.

(40) (a) Luo, C.; Guldi, D. M.; Imahori, H.; Tamaki, K.; Sakata, Y. *J. Am. Chem. Soc*. **2000,** *122*, 6535−6551. (b) Fukuzumi, S.; Imahori, H.; Yamada, H.; El-Khouly, M. E.; Fujitsuka, M.; Ito, O.; Guldi, D. M. *J. Am. Chem. Soc*. **2001,** *123*, 2571−2575. (c) Imahori, H.; Tamaki, K.; Guldi, D. M.; Luo. C.; Fujitsuka, M.; Ito, O.; Fukuzumi, S. *J. Am. Chem. Soc*. **2001,** *123*, 2607−2617. (d) Imahori, H.; Guldi, D. M.; Tamaki, K.; Yoshida, Y.; Luo, C.; Sakata, Y.; Fukuzumi, S. *J. Am. Chem. Soc*. **2001,** *123*, 6617−6628. (e) Imahori, H.; Tamaki, K.; Araki, Y.; Sekiguchi, Y.; Ito, O.; Sakata, Y.; Fukuzumi, S. *J. Am. Chem. Soc*. **2002,** *124*, 5165−5174.

(41) (a) Lindell, P. A.; Kuciauskas, D.; Sumida, J. P.; Nash, B.; Nguyen, D.; Moore, A. L.; Moore, T. A.; Gust, D. *J. Am. Chem. Soc*. **1997,** *119*, 1400−1405. (b) Carbonera, D.; Di Valentin, M.; Corvaja, C.; Agostini, G.; Giacometti, G.; Liddell, P. A.; Kuciauskas, D.; Moore, A. L.; Moore, T. A.; Gust, D. *J. Am. Chem. Soc*. **1998,** *120*, 4398−4405.

(42) Andersson, A.; Linke, M.; Chambron, J.-C.; Davidsson, J.; Heitz, V.; Sauvage, J.-P.; Hammarstrom, L. *J. Am. Chem. Soc*. **2000**, *122*, 3526−3527.